High Density, Vertically-Aligned Carbon Nanotube Membranes

Miao Yu, Hans H. Funke, John L. Falconer*, Richard D. Noble

Department of Chemical and Biological Engineering, University of Colorado

Boulder, CO 80309-0424

August 21, 2008

*Corresponding author: john.falconer@colorado.edu Ph: (303) 492-8005

Abstract

A method is presented to prepare high-density, vertically-aligned carbon nanotube (VA-CNT) membranes. The CNT arrays were prepared by chemical vapor deposition (CVD), and the arrays were collapsed into dense membranes by capillary-forces due to solvent evaporation. The average space between the CNTs after shrinkage was ~ 3 nm, which is comparable to the pore size of the CNTs. Thus, the interstitial pores between CNTs were not sealed, and gas permeated through both CNTs and interstitial pores. Nano-filtration of gold nanoparticles and N_2 adsorption indicated the pore diameters were approximately 3 nm. Gas permeances, based on total membrane area, were 1 to 4 orders of magnitude higher than VA-CNT membranes in the literature, and gas permeabilities were 4 to 7 orders of magnitude higher than literature values. Gas permeances were approximately 450 times those predicted for Knudsen diffusion, and ideal selectivities were similar to or higher than Knudsen selectivities. These membranes separated a larger molecule (triisopropyl orthoformate (TIPO)) from a smaller molecule (n-hexane) during pervaporation, possibly due to the preferential adsorption, which indicates separation potential for liquid mixtures.

Several studies have reported vertically-aligned, carbon nanotube (VA-CNT) membranes with high fluxes [1-3]. The nanotubes were sealed in a polymer or inorganic matrix, however, so that CNTs comprised less than 3% of the membrane permeation area; most of the membrane area was not available for permeation. Hinds *et al.* [1] prepared composite membranes with 6-7 nm (inner diameter) multi-walled CNTs by using polystyrene to fill the spaces between the CNTs. The flow velocities of molecules in their CNT membranes in pressure-driven permeation were 4-5 orders of magnitude higher than those calculated from fluid flow theory due to the smoothness of the CNT walls [4]. This is consistent with previous simulation results[5]. Holt *et al.* [2] grew vertically-aligned, dual-wall CNT membranes with much smaller pores (1.6 nm average) using a pre-deposited nano-catalyst (10-nm Al_2O_3, 0.3-nm Mo, 0.5-nm Fe) on a silicon wafer. They sealed the spaces between

the CNTs with silicon nitride that was deposited by chemical vapor deposition (CVD). They reported gas fluxes that were one to two orders of magnitude higher than those predicted by the Knudsen model, and ideal gas selectivities were similar to Knudsen selectivities for non-hydrocarbon gases and slightly higher than Knudsen selectivities for hydrocarbons. They also reported water fluxes that were 3 orders of magnitude higher than those calculated by the Hagen-Poiseuille equation. Kim *et al.* [3] used a different approach to prepare CNT membranes. They filtrated aligned, single-walled CNTs (1.2-nm average pore size) with a PTFE filter, and then sealed the space between the CNTs with polysulfone polymer by spin coating. Their membranes had ideal gas selectivities similar to Knudsen selectivities. Their membranes also had a CO_2/CH_4 separation selectivity equal to 1.6, whereas the single component selectivity was 0.6.

These composite membranes had low CNT porosity, and thus the fractions of the permeation areas that were CNTs were 2.7%, 0.5% and 0.079% in these three studies [1-3]. Therefore, although the fluxes through individual nanotubes were high, the fluxes per cm^2 of membrane area were limited because of the low porosity. In addition, the fabrication processes of the composite CNT membranes were complicated and thus expensive. In contrast to the above studies, which used CNT pores as transport pathways, Srivastava *et al.* [6] made a CNT filter from vertically-aligned CNT forests without a filler. Because their nanotubes were mostly blocked by catalyst particles, transport was in the interstitial spaces, which were approximately 20-30 nm across. In the current study, free-standing VA-CNT membranes with high CNT densities (~ 20% CNT porosity) were fabricated by shrinking free-standing VA-CNT arrays that were grown by CVD [7]. Since no filler was used, gases also permeated through the interstitial spaces between the CNTs. The diameters of both the CNT and the interstitial pores were approximately 3 nm (see below).

The membrane fabrication process is illustrated Fig. 1a. Vertically-aligned CNT forests were grown by water-assisted, CVD synthesis at 1020 K, as reported by Hata *et al.* [8] (see supporting information). Carbon nanotubes grew approximately linearly with growth time, and reached approximately 2 mm in length in 120 min (see supporting information Fig. S-1). The arrays used to prepare membranes were grown for 40 min and were 750 μm thick. Water etching at 1020 K, as described by Ci *et al.* [9] (see supporting information), was used after CVD to detach the CNT arrays and obtain free-standing layers. Figure 1b shows a SEM image of a detached, CNT forest after water etching at 1025 K for 15 min The procedure reported by Futaba *et al.* [7] was then used to make densely-packed, CNT forests by collapsing the CNT forests with capillary forces. They found that evaporation of solvents from between the CNTs shrank the layer to appropriately 5% of its

original size. In our study, the free-standing arrays were soaked in n-hexane, and the layers were dried at room temperature to collapse them. As indicated in Fig. 1c, the as-grown VA-CNT forest shrank to approximately 5% of its original area after n-hexane evaporation. The dense membranes were then mounted on silver-plated filters (5-μm pore size) that were embedded in nickel VCR gaskets (Swagelok), as shown in Fig. 1d. Gas and liquid permeations were measured by placing the membranes in standard VCR fittings.

The catalyst most frequently used for water-assisted CVD growth of VA-CNTs is 1~3 nm iron deposited on a 10~30 nm alumina layer [8,10-12]. The resulting pore sizes and the number of nanotube walls depend strongly on the iron thickness. For example, for 1-nm Fe/10-nm Al_2O_3 catalyst films, the CNT layers that formed have been reported to vary from 1-3 nm SWCNTs [8] to 5-nm DWCNTS [12]. A TEM of CNTs prepared in the current study (Fig. S-2) showed that that the inner pore diameters ranged from 2.2 to 4.7 nm, with an average of 3.6 ± 0.9 nm. This is consistent with Hata *et al*.'s results [8].

As shown by SEM imaging in Fig. 2a, the as-grown CNTs were aligned. After the CNT layer was collapsed by n-hexane evaporation, the CNTs were still aligned, but packed more densely (Fig. 2b). No cracks were seen, and the surfaces were smooth (Fig. 2c). Pore size distributions were calculated from N_2 adsorption and desorption at 77 K and the Barrett–Joyner–Halenda (BJH) method. As shown in Fig. 2d, two peaks, at approximately 3 and 30 nm, were seen for the as-grown CNT forest. These correspond to the CNT pores, which were estimated to be 3.6 nm from TEM measurements (see supporting information Fig. S-2), and the interstitial pores. The distance between the centers of CNTs in the as-grown CNT forest was estimated to be 28 nm (Table 1 & Fig. 1a) from the CNT porosity (~ 1%) and the average size of CNTs (~ 3 nm from N_2 adsorption/desorption). After shrinkage by solvent evaporation, the interstitial pores reduced to an average size of 2.8 ± 0.7 (std dev) nm with a range from 1.4 to 7 nm. This spacing is consistent with the average space between CNT centers (6 nm) calculated from the dense membrane density and the average CNT size. A comparison of the properties of the as-grown arrays and the dense membranes with CNT membranes in the literature is presented in Table 1.

Two advantages of these dense membranes are their CNT density is 8 to 270 times that of previous CNT membranes, and they do not contain a binder. Two studies [9,10] showed that water opened the CNT caps and etched the interface between CNTs and the Fe catalysts during water-assisted CVD growth. Therefore, the tops of our VA-CNT are expected to be opened by water etching. The substrates could be reused several times after detaching the arrays by water etching.

This indicates that most of the iron catalysts remained on the substrates and did not block the bottoms of the VA-CNTs. Reactive ion etching was used to slightly etch the top of a dense CNT membrane, but this did not change the gas flux, indicating the CNTs were already open on the top. Thus, etching was not necessary for this membrane preparation.

Hydrogen permeances were measured as a function of feed pressure for two dense membranes; the permeate pressure was held at 84 kPa. As shown in Fig. 3a, the H_2 permeance decreased with pressure drop. Permeance for viscous flow increases with feed pressure and is independent of feed pressure for Knudsen flow. Thus, neither viscous nor Knudsen flow dominates the transport across these membranes. The H_2 permeances were 450 times the values calculated for Knudsen diffusion (Fig. 3a). Simulations by Newsome and Sholl [13] predict significant enhancement of gas permeance through CNTs over Knudsen diffusion.

The single gas permeances decreased with pressure drop for six gases with molecular weights from 2 to 146 (Fig. 3b). This behavior is different from that expected for Knudsen flow, and Chen et al. [14] and Skoulidas et al. [5] reported that their simulations indicated that Knudsen behavior is not expected for CNT membranes. The ideal selectivities (H_2 relative to other gases) were similar to Knudsen for membranes 1 and 3, but higher than Knudsen for membrane 2 (Fig. 3c). Because membrane shrinkage is not completely controlled, membrane quality varied. Membrane 2 may have had a larger number of smaller pores that favor H_2 permeation. The H_2 and N_2 permeances decreased as the temperature increased for membrane 2 (Fig. 3d), and exhibited $T^{-1/2}$ dependence on temperature, which is the same as seen for Knudsen diffusion. Even though these dense CNT membranes exhibited single-gas selectivities higher than Knudsen values, no separation was seen at room temperature for several 50/50 mixtures (CH_4/CO_2, CO_2/H_2, CH_4/N_2) for pressure drops from 10 to 250 kPa. The high permeances (relative to Knudsen diffusion), decreasing permeance with pressure drop, and no separation selectivity indicate that transport though these dense CNT membranes is not Knudsen, even though the ideal selectivities and temperature dependence of permeance were similar to Knudsen values

Nitrogen permeabilities at room temperature through membrane 1 and CNT composite membranes from the literature are compared in Table 1. Nitrogen permeability ((flux × membrane thickness)/pressure drop) for the dense membrane, based on membrane permeation area (CNT pore area + interstitial area), is 1 to 4 orders of magnitude higher than N_2 permeabilities through CNTs in CNT composite membranes. The N_2 permeability is 3 to 7 orders of magnitude higher than those for CNT composite membranes based on total membrane area. Newsome and Sholl[13] found, using

molecular simulations, that surface resistance (resistance of entering and leaving pores) reduced CH_4 flux at room temperature for SWNTs (diameter 1.56 nm) that are shorter than 5 μm. Thus, surface resistance may lower the permeability (compared to thicker membranes) for the composite membranes in refs *(2)* and (*3)*.

The N_2 permeability for dense membranes (based on open permeation area) is 4 orders of magnitude higher than that for Kim *et al.*'s membrane[13]. Because they spin-coated a polymer to seal the space between their CNTs, some of their CNTs may not have been open, and thus not available for permeation; they did not use a procedure to open the CNTs. Hinds *et al.*'s membranes[13] had N_2 permeances similar to that predicted by Knudsen diffusion. Because most of their CNT pores were blocked by catalyst, their N_2 permeation area was probably smaller than the 2.7% of the total permeation area that they calculated. If a smaller permeation area were used to calculate N_2 permeability for the membranes prepared by Hinds *et al.*[1], the ratio of permeability of dense membrane to Hinds *et al.*'s membrane would be less than 160, which is the value calculated from Table 1. The dense CNT membranes have greater than 95% of their area (CNT pore area + interstitial pore area) available for permeation, whereas the CNT composite membranes used less than 3% of their membrane area for permeation. This leads to significantly higher permeabilities for the dense membranes (Table 1).

The maximum size of the pores in the dense membranes was estimated by filtering 3.2-nm gold nanoparticles in DI water (Purest Colloids Co.). Water with 12,800 ppb gold was introduced to the feed side of the membrane, which was pressurized to 184 kPa. The liquid filtrate was analyzed by inductively coupled plasma mass spectrometry. The filtrates for membranes M1 and M2 contained 72 and 35 ppb gold, respectively (Table 2). That is, more than 99% of the gold particles were rejected by dense CNT membranes. Because the gold particle size is comparable to the estimated pore size (from N_2 adsorption), the water flux decreased to 2 to 3% of the pure water flux (Table 2). The membranes were cleaned so that the water flux recovered after 30 min sonication in DI water.

Triisopropyl orthoformate (TIPO, 1.0 nm) was separated from n-hexane (0.43 nm) by a dense CNT membrane by pervaporation, which uses a liquid feed and vacuum on the permeate side. The permeate vapor was condensed in a liquid nitrogen trap and analyzed by GC. A dense CNT membrane separated TIPO from n-hexane with a separation factor (TIPO wt%/n-hexane $wt\%)_{permeate}$/(TIPO wt%/n-hexane $wt\%)_{feed}$) of approximately 3 for a 50wt%/50wt% feed mixture. Because both molecules are smaller than the membrane pore size, and TIPO has a much higher molecular weight, this separation may result from preferential adsorption of TIPO.

In summary, dense VA-CNT membranes have advantages over CNT composite membranes. Eliminating the spaces between CNTs in CVD grown CNT forests by collapsing the structure by solvent evaporation results in much higher CNT porosity (~ 20%). Because interstitial pores are comparable to CNT pore sizes (3 nm), no sealing materials were used so membrane fabrication was simplified, and additional permeation area was available. Gas diffusion through these membranes is not Knudsen; permeances are 2 orders of magnitude higher.

Supporting information available: experimental set-up and procedures, additional characterization, and membrane preparation.

Acknowledgment

We gratefully acknowledge support by the National Science Foundation Grant CBET-0730047.

References

1. Hinds, B.J. et al. Aligned multiwalled carbon nanotube membranes. *Science* **303**, 62-65 (2004).
2. Holt, J.K. et al. Fast mass transport through sub-2-nanometer carbon nanotubes. *Science* **312**, 1034-1037 (2006).
3. Kim, S., Jinschek, J.R., Chen, H., Sholl, D.S. & Marand, E. Scalable fabrication of carbon nanotube/polymer nanocomposite membranes for high flux gas transport. *Nano Lett.* **7**, 2806-2811 (2007).
4. Majumder, M., Chopra, N., Andrews, R. & Hinds, B.J. Nanoscale hydrodynamics - Enhanced flow in carbon nanotubes. *Nature* **438**, 44-44 (2005).
5. Skoulidas, A.I., Ackerman, D.M., Johnson, J.K. & Sholl, D.S. Rapid transport of gases in carbon nanotubes. *Phy. Rev. Lett.* **89**, - (2002).
6. Srivastava, A., Srivastava, O.N., Talapatra, S., Vajtai, R. & Ajayan, P.M. Carbon nanotube filters. *Nat. Mater.* **3**, 610-614 (2004).
7. Futaba, D.N. et al. Shape-engineerable and highly densely packed single-walled carbon nanotubes and their application as super-capacitor electrodes. *Nat. Mater.* **5**, 987-994 (2006).
8. Hata, K. et al. Water-assisted highly efficient synthesis of impurity-free single-walled carbon nanotubes. *Science* **306**, 1362-1364 (2004).
9. Ci, L.J., Manikoth, S.M., Li, X.S., Vajtai, R. & Ajayan, P.M. Ultrathick freestanding aligned carbon nanotube films. *Adv. Mater.* **19**, 3300-+ (2007).
10. Zhu, L.B., Xiu, Y.H., Hess, D.W. & Wong, C.P. Aligned carbon nanotube stacks by water-assisted selective etching. *Nano Lett.* **5**, 2641-2645 (2005).

11. Chakrabarti, S., Nagasaka, T., Yoshikawa, Y., Pan, L.J. & Nakayama, Y. Growth of super long aligned brush-like carbon nanotubes. *Jpn. J. Appl. Phys. 2* **45**, L720-L722 (2006).
12. Chakrabarti, S., Kume, H., Pan, L.J., Nagasaka, T. & Nakayama, Y. Number of walls controlled synthesis of millimeter-long vertically aligned brushlike carbon nanotubes. *J. Phys. Chem. C* **111**, 1929-1934 (2007).
13. Newsome, D.A. & Sholl, D.S. Influences of interfacial resistances on gas transport through carbon nanotube membranes. *Nano Lett.* **6**, 2150-2153 (2006).
14. Chen, H.B. & Sholl, D.S. Predictions of selectivity and flux for CH_4/H_2 separations using single walled carbon nanotubes as membranes. *J. Membr. Sci.* **269**, 152-160 (2006).

Table 1: Properties of CNT membranes

Membrane Properties	This study		Reference		
	As grown	Dense membrane	(1)	(2)	(3)
Average CNT inner diameter, nm	3.0	3.0	7.5	1.6	1.2
Thickness, μm	750	750	5	2	0.6
Morphology	—	CNT and interstitial pores	CNT/polymer composite	CNT/Si_3N_4 composite	CNT/polymer composite
Density, g/cm^3	0.010	0.21	—	—	—
CNT density, 10^{10} CNT/cm^2	14 *	290 *	6.0	25	7.0
Average distance between CNTs, nm	28	6	41	20	38
CNT volume occupancy, %	1	21	2.7	0.50	0.079
N_2 permeability based on open permeation area, 10^{-4} cm^3 (STP)·cm/(cm^2·s·atm)	—	17,800**	110	2,000	1.3
N_2 permeability based on total membrane area, 10^{-4} cm^3 (STP)·cm/(cm^2·s·atm)		17,000**	3.0	10	0.001

* Estimated from the N_2 adsorption/desorption measurements at 77 K

** Membrane 1 at a pressure drop of 200 kPa

Table 2: Removal of nano-gold particles from DI water

Membrane	Water flux, $kg/m^2 \cdot h \cdot bar$	Water flux with 12,800 ppb Au particles, $kg/m^2 \cdot h \cdot bar$	Au concentration in filtrate, ppb
M1	2,130	44	72
M2	2,740	80	35 ± 2

Figure Captions

Figure 1: Preparation of high density, vertically aligned carbon nanotube membranes. a) schematic representation 1) chemical vapor deposition of vertically-aligned CNT forest; 2) in-situ water etching to detach the CNT forest; 3) soaking and evaporating to densify CNT forest. b) SEM image of a VA-CNT forest detached by water etching. c) Photograph of a dense CNT membrane; white dotted lines indicate the original size of as-grown CNT forest. d) Photograph of a porous filter and a dense CNT membrane glued onto it.

Figure 2: a) SEM image of the cross-section of an as-grown CNT forest. b) SEM image of the cross-section of a dense CNT membrane (scale bar 1 μm). c) SEM image of the top surface of a dense CNT membrane (scale bar 100 μm) and magnified top surface in the inset SEM image (scale bar 5 μm). d) Pore size distribution of as-grown CNT forests and dense CNT membranes calculated from N_2 adsorption/desorption isotherms at 77 K.

Figure 3: Gas permeation through dense VA-CNT membranes: a) hydrogen permeance versus pressure drop for membranes M1 and M2; b) single gas permeances through membrane M1 versus pressure drop; c) ideal selectivity for three membranes (M1: open triangles; M2: open squares; M3: solid circles) at 50 kPa pressure drop. Line is Knudsen selectivity; d) hydrogen and nitrogen permeances through membrane M3 versus $T^{-1/2}$.

.

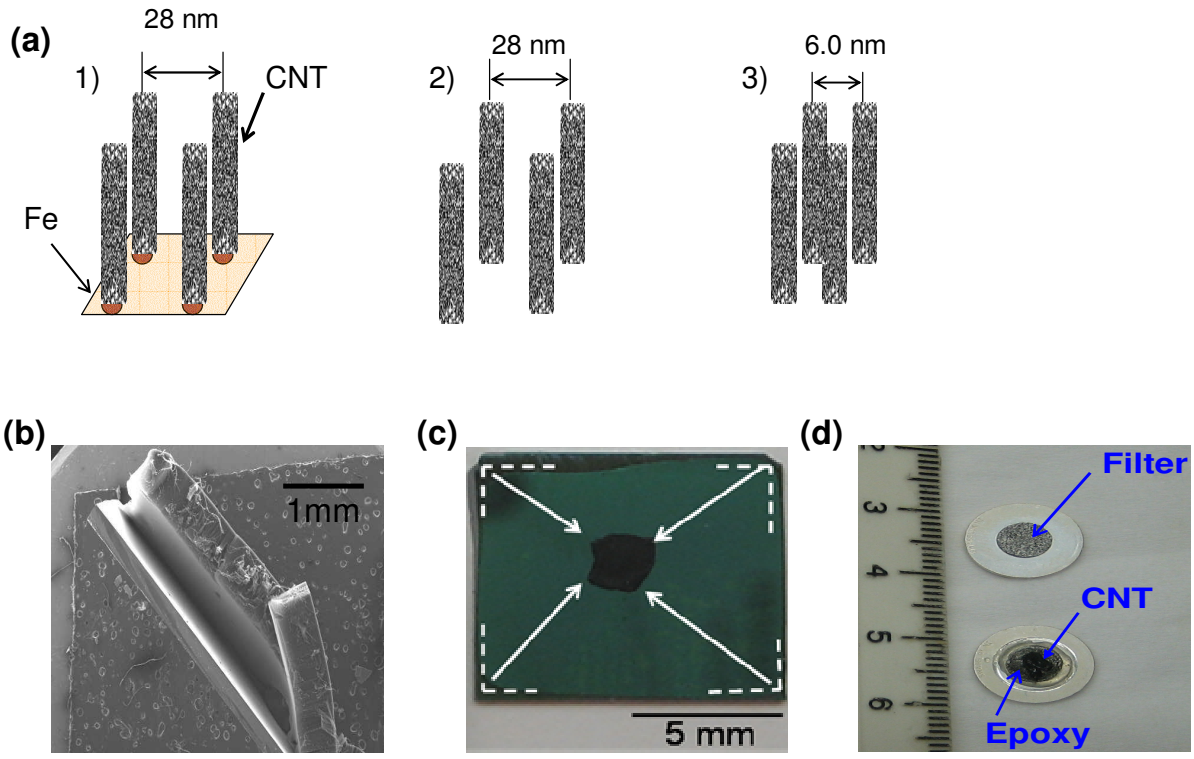

Figure 1: Preparation of high density, vertically aligned carbon nanotube membranes. a) schematic representation 1) chemical vapor deposition of vertically-aligned CNT forest; 2) in-situ water etching to detach the CNT forest; 3) soaking and evaporating to densify CNT forest. b) SEM image of a VA-CNT forest detached by water etching. c) Photograph of a dense CNT membrane; white dotted lines indicate the original size of as-grown CNT forest. d) Photograph of a porous filter and a dense CNT membrane glued onto it.

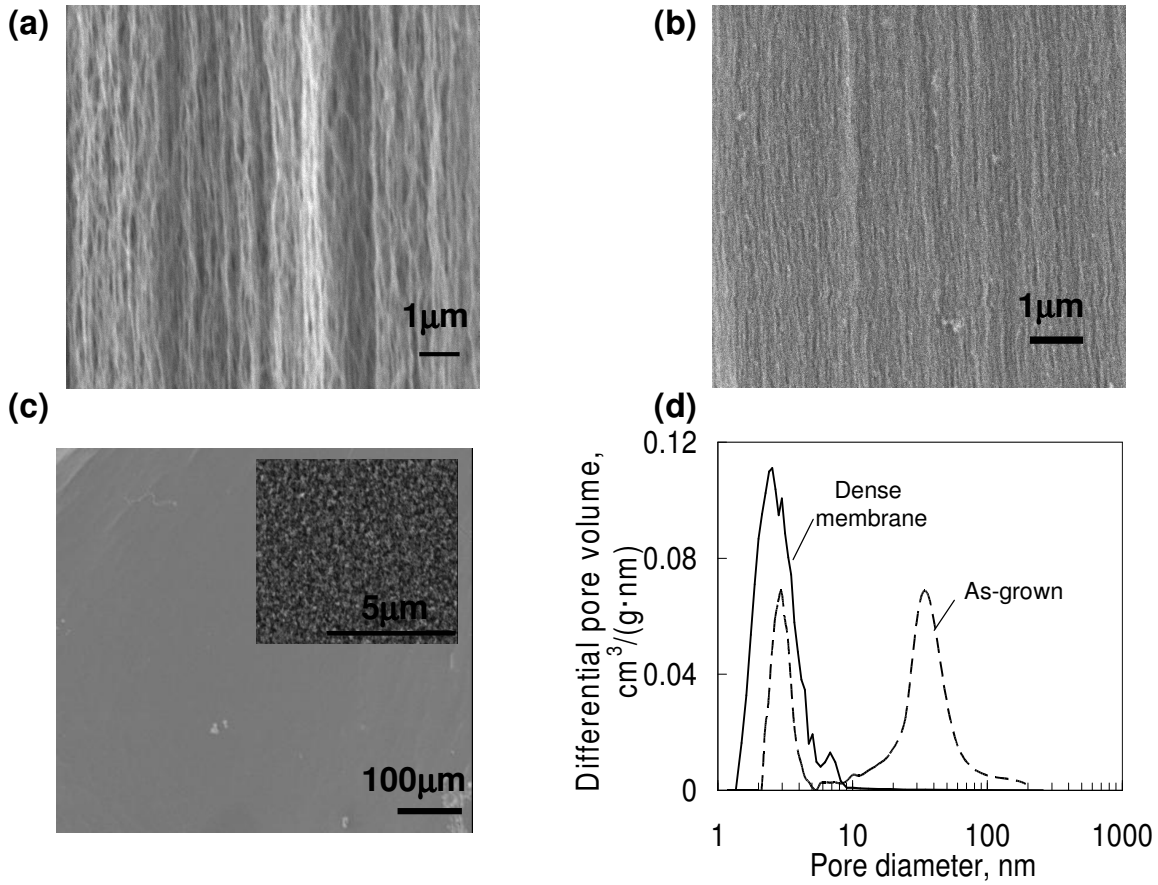

Figure 2: a) SEM image of the cross-section of an as-grown CNT forest. b) SEM image of the cross-section of a dense CNT membrane (scale bar 1 μm). c) SEM image of the top surface of a dense CNT membrane (scale bar 100 μm) and magnified top surface in the inset SEM image (scale bar 5 μm). d) Pore size distribution of as-grown CNT forests and dense CNT membranes calculated from N_2 adsorption/desorption isotherms at 77 K.

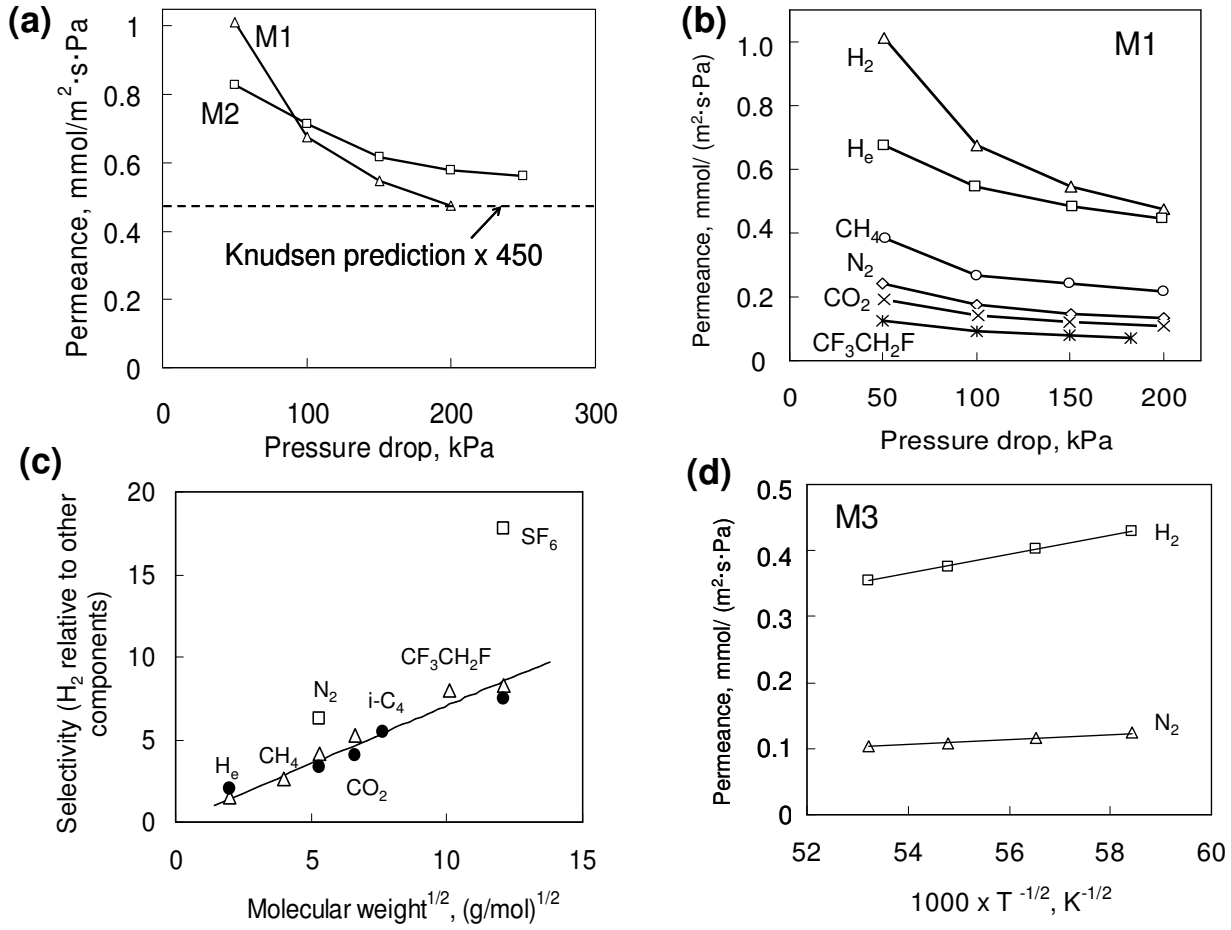

Figure 3: Gas permeation through dense VA-CNT membranes: a) hydrogen permeation at different pressure drop for 2 dense CNT membranes; b) single gas permeation through membrane M1; c) ideal selectivity for three membranes, membrane M1 (open triangle), membrane M2 (open square) and membrane M3 (solid circle) at 50 kPa pressure drop; solid line is Knudsen selectivity; d) permeation of hydrogen and nitrogen through membrane M3 at different temperature.

SUPPORTING INFORMATION

1. Growth of vertically-aligned carbon nanotube array

The growth procedure of vertically-aligned carbon nanotube arrays follows water-assisted highly efficient chemical vapor deposition (CVD) synthesis suggested by Hata *et al.* (*1*). Chemical vapor deposition (CVD) was conducted in a horizontal quartz tube (5.1 cm diameter and 90 cm long) housed in a Lindberg furnace. The catalyst thin films (1 nm Fe/ 10 nm Al_2O_3) were deposited on silicon wafer with 500 nm oxidation layer by sequential e-beam evaporation. At room temperature substrates were placed into the oven, and argon was introduced at 600 sccm to purge out the air. At the same time, start to heat the oven to 750 ^oC. When the oven temperature reached 350 ^oC, hydrogen (400 sccm) was introduced, and after 20 min (oven temperature, 660 ^oC) an argon stream (30 sccm) bubbled through a water bubbler to introduce small amount of water (~ 730 ppm) to the reactor. After another 10 min, oven temperature reached 750 ^oC and stabilized, ethylene (100 sccm) was introduced for a designated time for growth. In order to detach the as grown VA-CNT array easily, water etching process was applied after CVD growth, as suggested by Ci *et al.* (*2*). Specifically, after CVD the ethylene flow was stopped and argon flow rate decreased to 400 sccm and hydrogen to 270 sccm, and argon flow rate through water bubbler increased to 50 sccm (~2000 ppm). During the water etching process, the oven temperature kept at 750 ^oC, and the etching process lasted for 15 min. Figure S-1 shows growth kinetics of the VA-CNT arrays. Thickness of VA-CNT layers increases appropriately linearly with the growth time, and for all the membranes for shrinkage the growth time is 40 min, and thus a thickness of 750 μm.

2. Preparation of dense VA-CNT membranes

We used a similar VA-CNT array shrinking procedure as Futaba et al. (*3*). After detaching an as-grown VA-CNT array from the silicon substrate, it was soaked in organic solvents, such as n-hexane, for 30 min. The wet CNT array was dried at room temperature naturally and shrank on a silicon wafer. The shrunk membrane was then stored in a vacuum oven at 70 ^oC for 24 h for later N_2 adsorption/desorption measurements or making a membrane. After storing in vacuum oven for 24 h, the membrane was glued on a porous filter (5 μm pores) using epoxy, which was ready to use for gas permeation measurements.

3. Nitrogen adsorption/desorption

Appropriately 20 mg as-grown or shrunk VA-CNT arrays were used for adsorption in an Autosorb-1 (Quantachrome Corp. Model AS1-C-VP-RGA) system. Prior to each adsorption experiment, the sample was outgassed in vacuum at 473 K for about 2 h. Nitrogen

adsorption/desorption measurements were performed at 77 K, and BJH desorption and HK methods were used for mesopore size distribution and pore volume calculation and micropore size distribution and pore volume calculation respectively.

4. Single gas permeation measurements

A dead end system was used for single gas permeation measurements. A gas pressure regulator was connected to the gas cylinder before the membrane to adjust the gas pressure in the system and a pressure gauge was used to read the pressure. Gas flux through membranes was measured by a bubble flow meter.

5. Nano-gold particle filtration experiments

Figure S-3a shows the experimental set-up for nano-gold particle filtration measurements. Dense CNT membranes were connected to a liquid reservoir by standard VCR fitting, and the liquid was pressurized by N_2. The filtrated liquid at atmosphere pressure was collected by a small vial and analyzed by inductively coupled plasma mass spectrometry (ICP-MS). Figure S-3b and c show that after filtration the solution became clear in contrast with the feed red solution.

5. Liquid mixture separation by pervaporation

Liquid mixture pervaporation (liquid feed, vacuum on permeate side) was carried out at 300 K in a liquid recirculation system similar to that described previously *(4).* The dense CNT membrane was connected to a liquid pump by VCR fitting, and liquid circulated at a flow rate of 1 L/s. The permeate was collected in a liquid nitrogen trap, and a permeate sample was weighed every 1-2 h to determine the flux, and its composition was measured by gas chromatography (GC). The pressure was below 0.25 kPa on the permeate side.

References

1. K. Hata *et al.*, *Science* **306**, 1362 (2004).
2. L. J. Ci, S. M. Manikoth, X. S. Li, R. Vajtai, P. M. Ajayan, *Advanced Materials* **19**, 3300 (2007).
3. D. N. Futaba *et al.*, *Nature Materials* **5**, 987 (2006).
4. T. C. Bowen *et al.,* Microporous and Mesoporous Materials 71, 199 (2004).

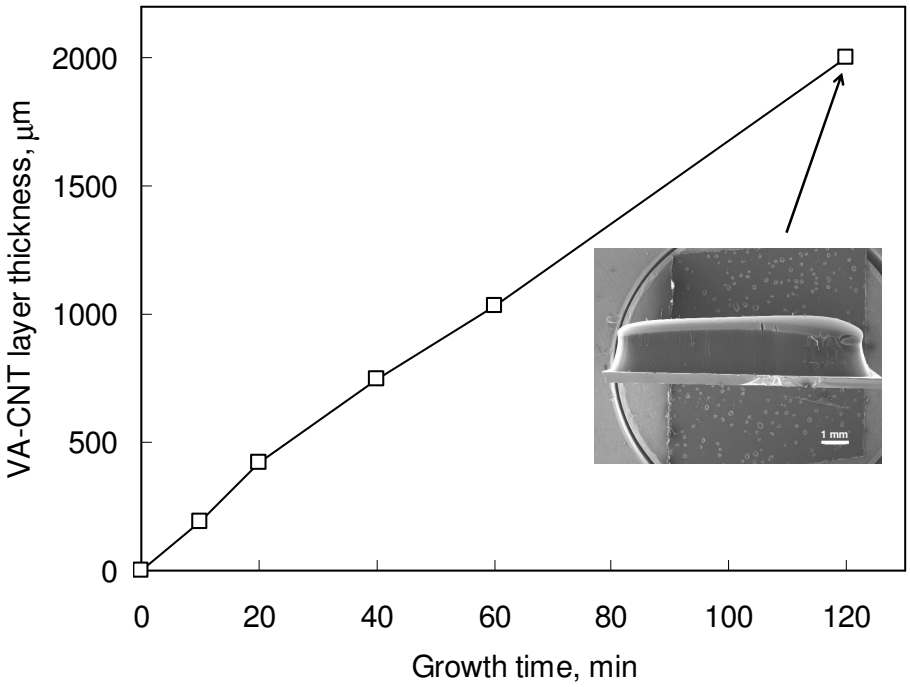

Figure S-1 Time evolution of VA-CNT array growth. Plot of the VA-CNT array thickness as a function of the growth time. Inset picture shows a sample of 2 mm thickness VA-CNT array.

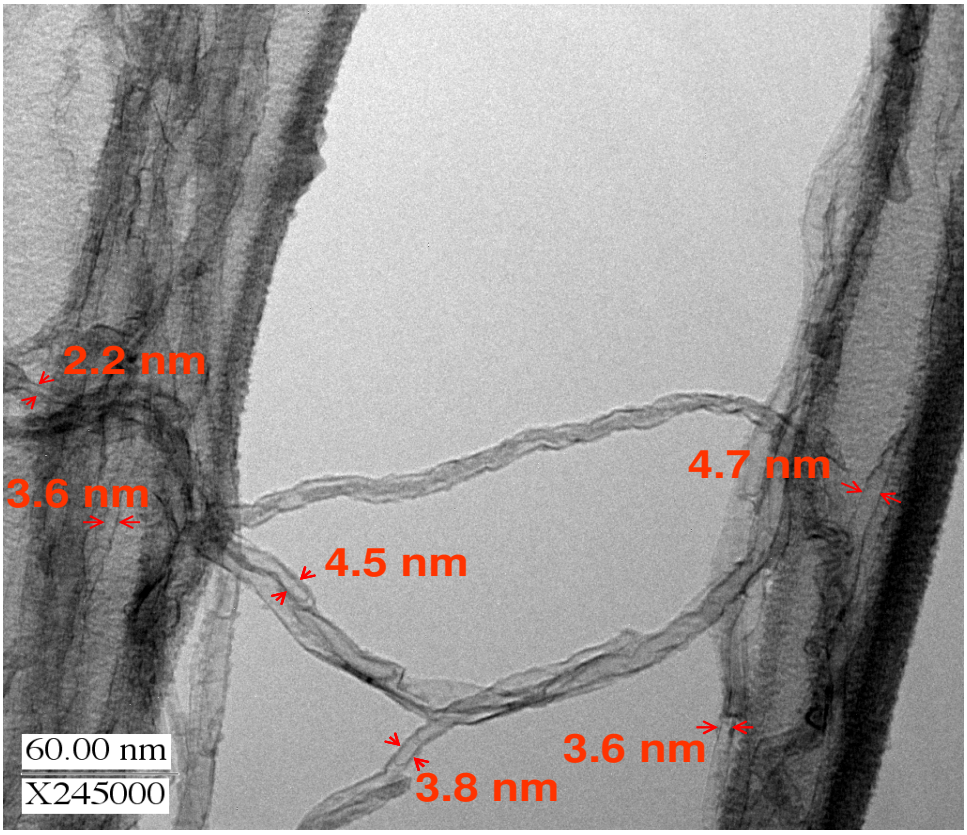

Figure S-2 Transmission electron microscopy (TEM) of carbon nanotubes grown from 1.0 nm Fe thin film.

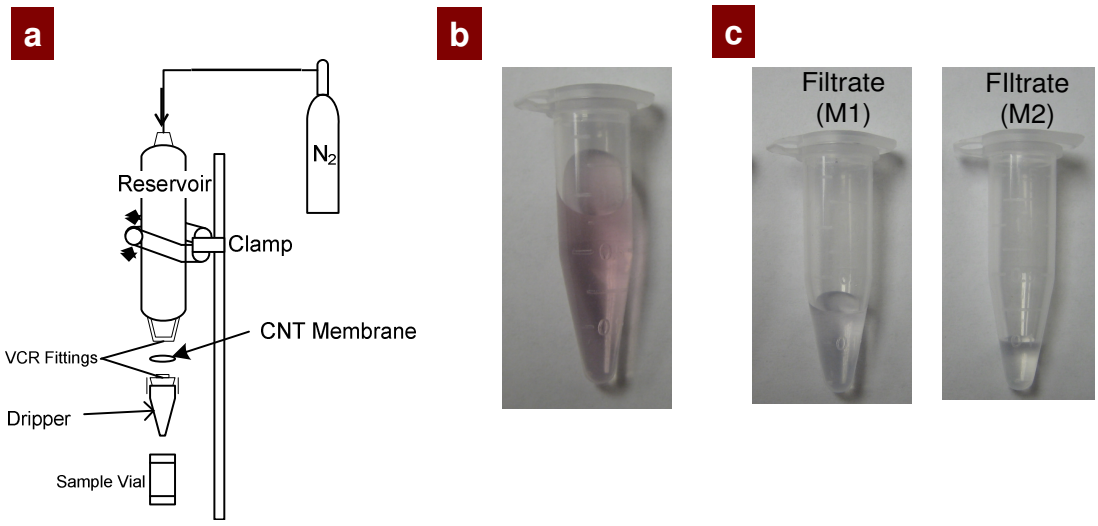

Figure S-3: Nano-gold particle removal measurements by pressurized liquid filtration. a) Experimental set-up for measuring filtration. b) Digital picture of feed solution of 12800 ppb nano-gold particles in DI water. c) Digital pictures of filtrates of two dense CNT membranes after membrane rejection.